Vibrationally Mediated Stabilization of Electrons in Nonpolar Matter

Jakub Med, Štěpán Sršeň, Petr Slavíček, A. Domaracka, S. Indrajith, P. Rousseau, M. Fárník, J. Fedor, J. Kočišek

Vibrationally Mediated Stabilization of Electron in Non-Polar Matter

Jakub Med,[†] Štepán Sršeň,[†] Petr Slavíček,[*,†,‡] A. Domaracka,[¶] S. Indrajith,[¶] P. Rousseau,[¶] M. Fárník,[‡] J. Fedor,[*,‡] and J. Kočišek[*,‡]

[†]*Department of Physical Chemistry, University of Chemistry and Technology, Technická 5, Prague 6, Czech Republic*

[‡]*J. Heyrovský Institute of Physical Chemistry v.v.i., The Czech Academy of Sciences, Dolejškova 3, 18223 Prague, Czech Republic*

[¶]*Normandie Univ., ENSICAEN, UNICAEN, CEA, CNRS, CIMAP, 14000 Caen, France*

E-mail: petr.slavicek@vscht.cz; juraj.fedor@jh-inst.cas.cz; jaroslav.kocisek@jh-inst.cas.cz

Abstract

We explore solvation of electrons in non-polar matter, here represented by butadiene clusters. Isolated butadiene supports only the existence of transient anions (resonances). Two-dimensional electron energy loss spectroscopy shows that the resonances lead to an efficient vibrational excitation of butadiene, which can result into almost complete energy loss of the interacting electron. Cluster-beam experiments show that molecular clusters of butadiene form stable anions, however only at sizes larger than 9 molecular units. We have calculated the distribution of electron affinities of clusters using classical and path integral molecular dynamics simulations. There is almost a continuous transition from the resonant to the bound anions with the increasing cluster size. The comparison of the classical and quantum dynamics reveals that the electron binding is strongly supported by molecular vibrations, brought about by nuclear zero point motion and thermal agitation. We also inspected the structure of the solvated electron, finding it well localized.

Graphical TOC Entry

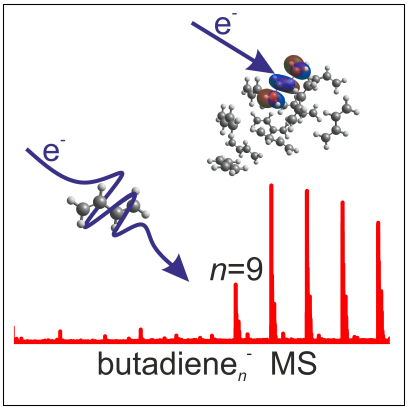

Keywords

American Chemical Society, LaTeX

Solvation of excess electron in neutral solvents has attracted the attention ever since its first observation, focusing mostly on polar solvents.[1] In liquid ammonia, the first medium in which the electron solvation was postulated in 1907,[2] the electron forms a cavity.[3] The situation is more complicated in liquid water, where its lifetime is only some 300 μs.[4] Most studies now agree that hydrated electron in water resides again in a cavity,[1] even though an interesting discussion on that subject has emerged in the last decade.[5–8] Solvated electron in a polar liquid is dominantly stabilized by electrostatic interactions – the electron is bound by a dipole of the polar solvent.[9] Much insight has been brought by inspecting anionic molecular clusters with the increasing number of monomeric units.[10–12] For example, isolated water molecule does not support the existence of a stable anion, however, already a water dimer does.[13] Also, even though the binding energy of the electron gradually increases,[14] the anion signal has a strong onset only above $n = 10$ water molecules.[15] This general trend was explained by simulations at both molecular and continuum level.[16,17]

The information on the binding of an electron in nonpolar clusters is much scarcer. Experimentally, one can distinguish two major approaches used. One is to collide neutral clusters with a beam of electrons or high-Rydberg atoms. This way, mainly small nonpolar targets such as O_2, CO_2, CS_2 were probed.[18–20] The vibrational Feshbach resonances, arising from the long-range electron-cluster interaction were shown to dramatically enhance the electron attachment cross section in a number targets. The second approach is to start with anionic clusters and probe the electron binding by photoelectron spectrocopy. Here, the attention focused mainly on clusters of aromatic molecules, such as benzene,[21] hexafluorobenzene[22] or polyaromatic hydrocarbons.[23,24] These works emphasized the role of electron localization/delocalization,[25] role of correlation bound states in the excess electron binding[22] or the solvation energetics.[21] In the latter case,[21] the continuous increase in the electron detachment energy with the clusters size up to the bulk limit has been observed.

Here we focus on the binding of electrons in non-polar matter represented by a butadiene molecule and its clusters. Butadiene has zero dipole moment, however, both its non-negligible polarizability and vibrations (e.g., via presence of IR active modes) can significantly influence electron binding. Therefore, it is interesting to find out the critical size of the cluster capable to capture the excess electron and whether the existence of an anion is supported at all. It is known that the lowest anion state in isolated butadiene is a resonance, lying 0.62 eV above the continuum limit.[26] As we show below, the clustering allows for almost continuous observation of the transformation from resonant to bound state.

Apart from the conceptual interest in electronic binding, there is also a practical interest in the questions posed above. The problem is e.g. relevant in the context of static electricity and the storage of the extra charge in non-polar matter.[27] Surprisingly, the molecular details of static electricity are far from being understood at the moment.[28] Charged butadiene can be in fact seen as molecular realization of electrets, dielectric materials with a quasi-permanently embedded static electric charge. Most electrets are made from synthetic polymers, materials with a very similar constitution to butadiene. The butadiene clusters, if binding the electrons, can be considered nanoelectrets, similar to the nanomagnets.[29]

We first explored the formation of the resonance in isolated molecule and the induced vibrational motion by employing 2D electron energy loss spectroscopy (Fig. 1). Here the electron with a controlled incident energy E_i (vertical axis) collides with the molecule and residual energy E_r of the ejected electron is recorded. The electron energy loss $\Delta E = E_i - E_r$ (horizontal axis) reflects the energy transferred to the molecule. The intensity cuts along the horizontal lines (Fig. 1b) are traditional electron energy loss spectra and reveal which vibrations are excited. The mode numbering follows the one used in Ref. 30. The intensity cuts along the vertical lines (Fig. 1c) correspond to the excitation functions of individual vibrations. The 2D spectrum is well in line with earlier studies of electron-butadiene collisions that used either electron transmission spectroscopy[26] or standard energy loss spectroscopy.[30,31]

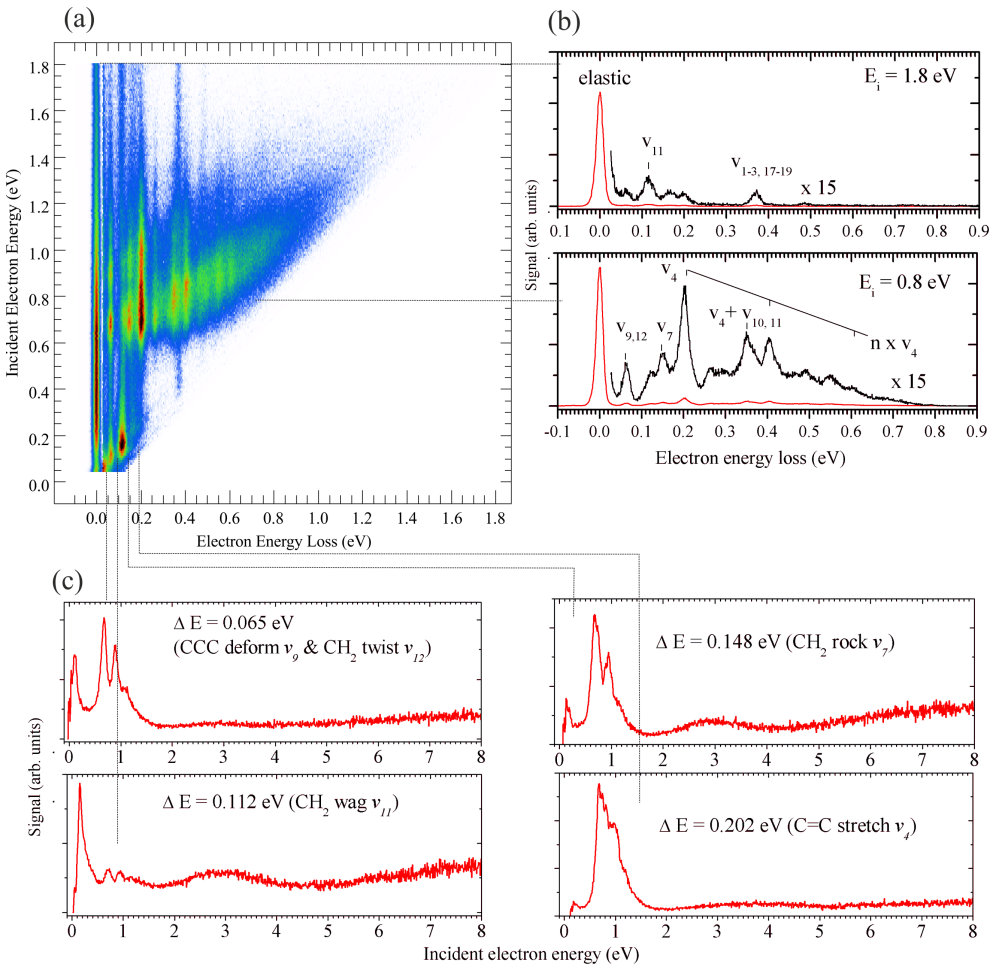

Figure 1: **(a)** Two-dimensional electron energy loss spectrum of 1,3-butadiane. **(b)** Electron energy loss spectra at two different incident energies (≡ horizontal intensity cuts) **(c)** Excitation curves of four selected energy losses (≡ vertical intensity cuts, recorded separately in longer energy range).

We can make several observations from the spectra. First, some vibrations are strongly excited at the threshold, as soon as the electron has enough energy to do so. In the 2D spectrum, this is manifested as dots just above the diagonal $E_i = \Delta E$. The probability of the electron-impact vibrational excitation is in the Born approximation proportional to the same matrix element as the infrared (IR) absorption intensity,[32,33] the intensity of the threshold excitation thus reflects the IR activity of the given mode. The second dominant feature in the 2D spectrum is the overall excitation enhancement between 0.6 and 1.2 eV incident energy. This is caused by the formation of the $\pi_1^*(^2A_u)$ resonance. Formation of

such a temporary anion induces a motion of nuclei on the potential energy surface. When the electron detaches in a different nuclear geometry than in its neutral equilibrium, the molecule is left vibrationally excited. The second π^* resonance ^2B_g is visible around 3 eV in the separately recorded excitation curves shown in Fig. 1c. All the vibrational modes that are excited by the π_1^* electronic resonance show a pronounced boomerang vibrational structure with the approximate spacing of 200 meV. It reflects the dominant vibrational motion on the temporary anion surface, in this case it is clearly the C=C stretch anion vibration.[26,30] Indeed, the comparison of the on-resonance (0.8 eV) and off-resonance (1.8 eV) energy loss spectra (Fig. 1b) shows that the resonance formation mainly enhances the C=C stretch (v_4, 202 meV) and its overtones and combination vibrations. There is a certain near-diagonal pattern visible in the resonant region. This is a well-known shift of the maxima of boomerang oscillation peaks with increasing vibrational excitation quantum.[34]

In the resonance region, one can observe a wide span of energy losses, where the electrons are emitted with up to a complete energy loss. These slow electrons are signature of an efficient intramolecular vibrational redistribution (IVR) on the resonant surface, where the energy is randomized over the vibrational degrees of freedom.[35,36] Such electron thermalization upon the collision with the butadiene monomer unit may strongly influence the electron binding in clusters.

The electron attachment to clusters was experimentally probed by colliding a beam of neutral butadiene clusters with a beam of free electrons and recording the resulting anion mass spectra. Fig. 2a shows sum of these mass spectra in the electron energy range 0.5-12.5 eV. There is only a progression of intact $[(\mathrm{But})_n]^-$ clusters with the onset at $n = 9$ and maximum already at $n = 10$. For anionic clusters with more than 10 units, the intensity of the peaks in the progression slowly decreases. Additionally, we can see weak signals for some small clusters such as $[(\mathrm{But})_4]^-$.

What is a reason for the sharp onset of the cluster size distribution? A possible explanation might be that the anion spectrum reflects the distribution of the neutral clusters in

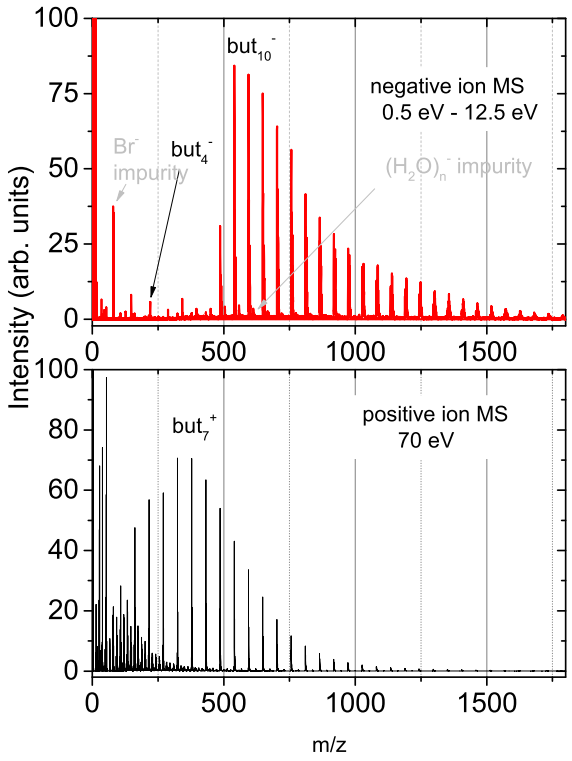

Figure 2: MS of negative ions formed after electron attachment to neutral butadiene clusters (top) and MS of positive ions after electron ionization (70 eV) of the clusters at the same expansion conditions (bottom).

the beam. However, it has been shown in numerous cases[37–39] (mainly by the soft ionization techniques) that the supersonic expansion produces a broad log-normal size distribution with small clusters always present in the beam. This is confirmed in the present case by positive ionization mass spectrum (Fig 2b) showing the $[(\mathrm{But})_n]^+$ cluster distribution with maximum at $n = 7$. Even though the positive ionization can induce rather large fragmentation,[40] the difference between positive and negative ion cluster distribution is not expected to be so large.[37,41] The neutral beam certainly contains clusters with $n < 9$. Our interpretation therefore is that the smaller clusters simply do not attach electrons, or their electron autodetachment lifetime is much shorter than the detection time in the present experiment (tens of microseconds).

In order to interpret this behaviour, we computationally explored the electron affinities on the manifold structures of butadiene clusters. As the first step, we have optimized the

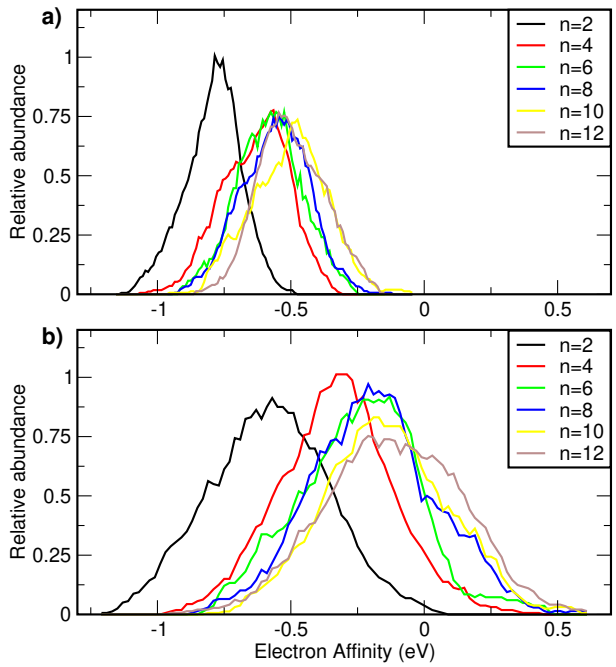

Figure 3: Vertical electron affinities (LC-wPBE/6-31+g*) of clusters with n butadiene molecules (n from 2 to 12), calculated along MD simulations: **(a)** with classical trajectories obtained with the DFTB interaction potential. **(b)** with path-integral simulations with generalized Langevin equation (PI-GLE).

structures of neutral and anionic clusters with $n = 2$ to $n = 12$ sizes. The corresponding geometries and adiabatic and vertical electron affinities (AEA and VEA) are shown in the Supporting Information, Table S1. Much more information is brought by inspecting the electron affinity distribution along trajectories from molecular dynamics simulations. Fig. 3a shows the histogram of VEAs evaluated for each cluster size for 100 geometries from classical MD simulations performed for 2 ns at 100 K. The right edge of such histogram corresponds to AEA for a given cluster size. The center of such histogram should intuitively correspond to VEA (listed in the Supporting Information), however, we observe a certain shift of this maximum to the higher values of the vertical electron affinity. Nevertheless, even for the largest clusters, neither the VEA or the AEA reach the positive value. Being it for classical mechanics, the clusters do not support the existence of the anionic clusters in this range of sizes.

As detailed in Methods, the VEAs are calculated using a ΔKS approach, meaning that

we calculate the electron affinity as a difference of the Kohn-Sham energy for the anion and the neutral molecule. This is justified only for bound anions, i. e. positive VEA values. Resonances (negative AEA values) can be reliably described by scattering calculations or by a number of approaches using conventional quantum chemical codes together with stabilization techniques.[42–45] DFT-based techniques were suggested as well.[46,47] However, all these would be impractical for large systems studied in the present work. The physical meaning of the negative ΔKS values is questionable, since we lack the basis set for the continuum part of the wavefunction. In any case, our only conclusion from the values in Fig. 3a is that all cluster sizes support only resonances and not stable anions.

The situation changes when we take into account the quantum nature (zero point motion) of nuclei. Fig. 3b shows the size evolution of the VEA distribution for the quantum (PI-GLE) simulations. These are the most realistic calculations when it comes to the comparison with the experiment. Clearly, the coupling between molecular vibrations and electron affinity of the clusters is much more pronounced here. The VEA is substantially shifted to the higher values of vertical electron affinity with respect to the classical simulations, by some 0.3-0.4 eV. We can now observe that for the largest clusters, the VEA approaches zero value. More importantly, the tail of the distribution extends to the positive values and the electrons are thus captured at many geometries. The vibrationally-induced shift of VEA is remarkable and we typically do not observe its analogue for the polar molecules. Clearly, the electronic stability is brought about by the vibrational motion.

Several effects contribute to this stabilization. The first is that already for an isolated butadiene, most of the deformations of the molecule lead to a decrease of its vertical electron affinity. This is demonstrated in Fig. S2 in the Supporting Information, showing the scans of anion and neutral energies along the normal modes. The second effect is the transient appearance of dipole moments along the IR-active vibrations. The third effect is provided by a cluster environment, where the vibrating anion can effectively decrease its excess energy by intermolecular vibrational redistribution. The spatial extend of nuclear wave packets

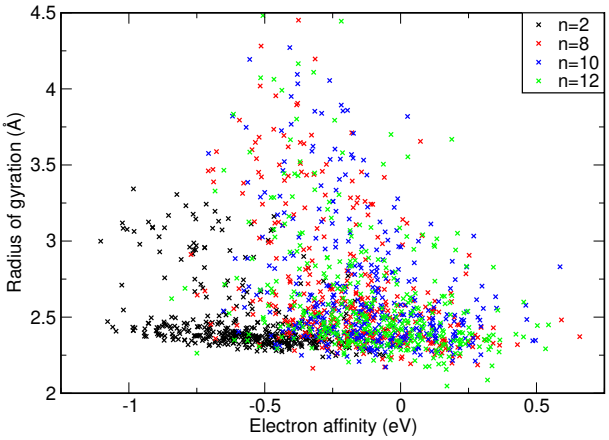

Figure 4: Radius of gyration of the unpaired electron of various-size clusters plotted against the electron affinity. Black crosses show clusters with two butadiene units. Read, blue and green crosses show clusters with 8, 10 and 12 butadiene units, respectively.

in quantum simulations magnifies all these effects. Finally, the neighboring molecules also stabilize the anion via an electronic polarization.

We also note that the width of the distributions (Fig. 1) converge faster than the VEA itself. The width is related to the reorganization energy of the system via the Marcus relation, i. e. the difference between the energy of the anion in its neutral geometry and in its anionic energy. For polar solvents, the solvent reorganization energy gradually increases (e.g. [41]). In the present case, the solvent reorganization energy does not seem to depend on the cluster size.

As a byproduct of the calculations, we can elucidate the question of the electron localization. Fig. 4 shows the distribution of the radius of gyration for anionic clusters. For positive VEA values, the gyration radii are small, which means that the electron is well localized. Fig. S1 in the Supporting Information demonstrates that the excess electron is localized on specific butadiene unit. The situation thus corresponds to a solvated valence anion, rather than to a solvated electron occupying a cavity or to a polarization-bound diffuse electron.

We can now interpret the experimental results in the light of the above calculations. Small anionic clusters are electronically unstable and their very existence is not supported. At some threshold cluster size, there are geometries capable to capture the electron or in

other terms, there are vibrational states below the ionization limits. The stability of the clusters increases with the increasing cluster size yet at the same time the abundance of the neutral cluster precursors decreases with increasing cluster size. We observe the peak maximum at butadiene decamer as a net result. Placing the threshold size for 9 butadiene units is in a good agreement with present calculations.

The role of vibrationally mediated binding becomes even more interesting, if we consider the attachment in the cluster as a stepwise process. As we have shown, the electron collision with a monomer leads to its efficient vibrational heating and ejection of a near-thermal electron. If this happens in a cluster, this doorway step right away enhances the process responsible for its stabilization, since it triggers the molecular vibrations. Still, the cluster has to be large enough in order to be able to bind this electron.

The present results can be brought into context with previous works on nonpolar clusters. The first aspect is the observation of minimal clusters size supporting the additional electron. If the molecular constituent supports a stable anion, the negative clusters are observed down to the monomer size.[25,48,49] Otherwise, the anion distribution has a sharp onset at certain size n,[21,50,51] similar to the present case.

Somewhat special case is a carbon dioxide, where stable $(CO_2)_n^-$ clusters were observed down to $n = 4$ or even to $n = 2$.[48,52–54] CO_2 monomer has a virtual state which becomes vertically bound upon bending, the geometry distortion stabilizes the small anionic clusters.[55] The second aspect is the binding mechanism. The dominant role is usually ascribed to the molecular polarizability.[56,57] The role of vibrations has been stressed only in connection with vibrational Feshbach resonances.[20,56] The present stabilization mechanism is different: the spatial extent of the nuclear wavepacket is equivalent to larger distortion of the molecular framework, which leads to its higher electron affinity. The nuclear quantum effects have recently attracted a lot of attention,[58] the present study points to yet another manifestation of these effects.

In conclusion, we have shown that relatively large ($n > 8$) butadiene aggregates are

needed to support the existence of bound anions. For smaller systems, the lowest anion states are resonances. Such resonances can further serve as doorway states for stable molecular anions of larger clusters. The remarkable finding is that the anionic clusters owe their existence to the coupling between electronic and nuclear motion, clusters in their minimal geometries have always negative electron affinity.

Present work can be regarded as nanoscale realization of the electrets. Electrets are now investigated as a possible energy harvesting and storage materials. It has been e.g. shown that charge storage can be achieved for years in silicon dioxide/nitride thin films.[59] Here we demonstrated that there exist bottom limit for scaling electret charge storage devices which is elucidated by experiment and theoretical modelling. The present study demonstrate importance of the vibrational energy redistribution and charge localization in the nanoelectrets. It would be interesting to explore the lifetime of the anions with respect to cluster size or effects of the substrate on the electron attachment process, which can be directly related to the charge storage properties of nanoelectrets.

Experimental methods

The 2D electron energy loss spectrum is a collection of 160 constant incident energy loss spectra that were recorded on the electrostatic electron spectrometer.[60,61] The incident electron beam, produced by a hemispherical electron monochromator, interacts with the effusive molecular beam of 1,3-butadiene and the scattered electrons are analyzed by a hemispherical electron analyzer. The scattering angle has been fixed at 135 degrees. The electron energy resolution in the energy loss mode was approximately 18 meV (combined resolution of monochromator and analyzer). The energy scale was calibrated on the 2^2S resonance in helium (19.365 eV).

The cluster experiments were carried out using CLUB (Cluster Beam) experimental setup in the negative ion detection mode.[62,63] We prepared beam of butadiene clusters by expansion

of pure (Messer 99.3%) 1,3-butadiene gas at expansion pressure 1.5 bar through 90 μm nozzle heated to temperature 55 °C to prevent condensation. The molecular beam was crossed by beam of low energy electrons 1.5 m downstream. Product anions were analyzed using 0.95 m long reflectron time-of-flight mass spectrometer. Cumulative negative ion mass spectra representing fragmentation of cluster anions upon electron attachment were obtained as a sum of 25 mass spectra measured at individual electron energies in 0.5-12.5 eV range (0.5 eV step). The negative ion MS were supplemented by measurement of single energy positive ion mass spectrum at energy of electrons 70 eV, acquired at the same expansion conditions.

Theoretical methods

Butadiene is a flexible system and therefore (i) it is difficult to find optimal structure for larger clusters due to a large number of distinct minima (ii) the optimal structure is not representative of the typical structure when vibrations are take into account. We have therefore sampled 100 geometries from MD simulations. We used finite temperature MD simulations at 100 K. At this temperature, butadiene does not evaporate within the simulation time yet it allowed some flexibility. The first type of simulations were classical MD simulations using Nosé-Hover thermostat. The equations of motion were integrated with Velocity Verlet integrator, using a timestep of 0.51 fs. The forces were calculated on-the-fly, using DFTB method with GD3 dispersion correction.[64,65] The second type of simulations accounted for nuclear quantum effects. We used path integral MD simulations, accelerated with a so called quantum thermostat based on the Generalized Langevin equation.[66] With this setup, even 4 beads are enough to achieve reasonable densities covering zero point delocalization for electronic spectra.[67,68] We have then selected 400 random points from the total 1000 ps trajectory for different cluster sizes comprising of 2, 4, 6, 8, 10 and 12 butadiene molecules. For these clusters, the electron affinities and radius of gyration were calculated along the

trajectory, i. e. we have used the reflection principle approach.

The electron affinities were calculated with density functional theory, using its long-range corrected variant.[69] In particular, we have used the LC-ωPBE functional[70] and the 6-31+g* basis set, using ΔKS approach, i. e. VEA=E(anion)-E(neutral). We fixed the ω parameter in the LC-ωPBE method by the process of optimal tuning of the range separated functional.[71,72] This is based on choosing the ω parameter such that we enforce the ionization potential theorem,[73] equating the orbital energy of the HOMO electron with ΔKS value of the ionization energy (the ionization potential theorem can be regarded as a DFT analogue of Koopmans's theorem). Here, we equate the SOMO orbital energy of the molecular anion with the ionization energy for several clusters with a positive electron affinity. We ended up with ω=0.30 bohr^{-1} as a reasonable compromise, used for all the calculations.

As an alternative, we have also used a simple estimate for negative VEAs as proposed by Tozer and De Proft[46] based on generalized gradient approximation (GGA) Kohn-Sham density functional theory

$$VEA = -(\varepsilon^{GGA}_{LUMO} + \varepsilon^{GGA}_{LUMO}) - VIE^{GGA} \tag{1}$$

where ε^{GGA}_{LUMO} and ε^{GGA}_{HOMO} are the frontier orbital energies of the neutral system and VIE^{GGA} is the vertical ionization energy of the neutral system. We have used the BLYP functional in our study. This formula provides a similar values for the vertical electron affinity as the ΔKS approach, see the Supporting Information.

Knowing the (normalized) electron density ρ of the extra electron, we have calculated the effective size of the solvated electron defined by its radius of gyration:

$$R_g = \sqrt{\int r^2 \rho(r) dr} \tag{2}$$

Gaussian09 package (revision D.01)[74] was used for the electron affinity calculations. The DFTB+ code was used for the ground state calculations.[64] All the MD calculations were

performed in our in-house ABIN code.[75]

Acknowledgement

The support by the Czech Science Foundation, projects no. 18-16577S (P.S. and J.M.), 19-01159S (J.K.) and 17-04844S (J.F.) are gratefully appreciated. J.K., S.I. and A.D. acknowledge the support by Czech-French cooperation programme PHC Barrande, project 7AMB17FR047, (Fr) 38079PL. J. M. is International Max Planck Research School student. Part of the calculations were done on the IT4I, project number OPEN-15-42.

Supporting Information Available

Supporting Information contains table with calculated vertical and adiabatic electron affinities, figure with electron densities of selected cluster structures, figure showing evolution of electron affinity along normal vibrational modes and cartesian coordinates of the optimized structures of neutral ground state butadiene clusters.

References

(1) Herbert, J. M.; Coons, M. P. The Hydrated Electron. *Annual Review of Physical Chemistry* **2017**, *68*, 447–472.

(2) Kraus, C. A. Solutions OF Metals in Non-Metallic Solvents; I. General Properties of Solutions of Metals in Liquid Ammonia. *Journal of the American Chemical Society* **1907**, *29*, 1557–1571.

(3) Jortner, J. Energy Levels of Bound Electrons in Liquid Ammonia. *The Journal of Chemical Physics* **1959**, *30*, 839–846.

(4) Walker, D. C. The Hydrated Electron. *Q. Rev. Chem. Soc.* **1967**, *21*, 79–108.

(5) Larsen, R. E.; Glover, W. J.; Schwartz, B. J. Does the Hydrated Electron Occupy a Cavity? *Science* **2010**, *329*, 65–69.

(6) Jacobson, L. D.; Herbert, J. M. Comment on "Does the Hydrated Electron Occupy a Cavity?". *Science* **2011**, *331*, 1387–1387.

(7) Turi, L.; Madarász, Á. Comment on "Does the Hydrated Electron Occupy a Cavity?". *Science* **2011**, *331*, 1387–1387.

(8) Larsen, R. E.; Glover, W. J.; Schwartz, B. J. Response to Comments on "Does the Hydrated Electron Occupy a Cavity?". *Science* **2011**, *331*, 1387–1387.

(9) Jordan, K. D.; Wang, F. Theory of Dipole-Bound Anions. *Annual Review of Physical Chemistry* **2003**, *54*, 367–396.

(10) Coe, J. V.; Earhart, A. D.; Cohen, M. H.; Hoffman, G. J.; Sarkas, H. W.; Bowen, K. H. Using cluster studies to approach the electronic structure of bulk water: Reassessing the vacuum level, conduction band edge, and band gap of water. *J. Chem. Phys.* **1997**, *107*, 6023–6031.

(11) Verlet, J. R. R.; Bragg, A. E.; Kammrath, A.; Cheshnovsky, O.; Neumark, D. M. Observation of Large Water-Cluster Anions with Surface-Bound Excess Electrons. *Science* **2005**, *307*, 93–96.

(12) Lietard, A.; Verlet, J. R. R. Selectivity in Electron Attachment to Water Clusters. *J. Phys. Chem. Lett.* **2019**, *10*, 1180–1184.

(13) Chen, H.-Y.; Sheu, W.-S. Dipole-Bound Anion of Water Dimer: Theoretical Ab-Initio Study. *The Journal of Chemical Physics* **1999**, *110*, 9032–9038.

(14) Lee, G. H.; Arnold, S. T.; Eaton, J. G.; Sarkas, H. W.; Bowen, K. H.; Ludewigt, C.; Haberland, H. Negative Ion Photoelectron Spectroscopy of Solvated Electron Cluster

Anions, (H2O)n- and (NH3)n-. *Zeitschrift für Physik D Atoms, Molecules and Clusters* **1991**, *20*, 9–12.

(15) Knapp, M.; Echt, O.; Kreisle, D.; Recknagel, E. Electron Attachment to Water Clusters Under Collision-Free Conditions. *The Journal of Physical Chemistry* **1987**, *91*, 2601–2607.

(16) Barnett, R. N.; Landman, U.; Cleveland, C. L.; Jortner, J. Electron Localization in Water Clusters. II. Surface and Internal States. *The Journal of Chemical Physics* **1988**, *88*, 4429–4447.

(17) Jortner, J. Dielectric Medium Effects on Loosely Bound Electrons. *Molecular Physics* **1962**, *5*, 257–270.

(18) Matejcik, S.; Kiendler, A.; Stampfli, P.; Stamatovic, A.; Märk, T. D. Vibrationally Resolved Electron Attachment to Oxygen Clusters. *Phys. Rev. Lett.* **1996**, *77*, 3771–3774.

(19) Leber, E.; Barsotti, S.; Fabrikant, I. I.; Weber, J. M.; Ruf, M.-W.; Hotop, H. Vibrational Feshbach Resonances in Electron Attachment to Carbon Dioxide Clusters. *The European Physical Journal D - Atomic, Molecular, Optical and Plasma Physics* **2000**, *12*, 125–131.

(20) Barsotti, S.; Leber, E.; Ruf, M.-W.; Hotop, H. High Resolution Study of Cluster Anion Formation in Low-Energy Electron Collisions with Molecular Clusters of CO_2, CS_2, and O_2. *International Journal of Mass Spectrometry* **2002**, *220*, 313 – 330, Van der Waals Clusters and Their Ions.

(21) Mitsui, M.; Nakajima, A.; Kaya, K. Negative Ion Photoelectron Spectroscopy of $(\text{Benzene})_n$ (n=53-124) and $(\text{Toluene})_n$ (n=33-139): Solvation Energetics of an Excess Electron in Size-Selected Aromatic Hydrocarbon Nanoclusters. *The Journal of Chemical Physics* **2002**, *117*, 9740–9749.

(22) Rogers, J. P.; Anstöter, C. S.; Bull, J. N.; Curchod, B. F. E.; Verlet, J. R. R. Photoelectron Spectroscopy of the Hexafluorobenzene Cluster Anions: $(C_6F_6)_n^-$ (n = 1–5) and $I^-(C_6F_6)$. *The Journal of Physical Chemistry A* **2019**, *123*, 1602–1612.

(23) Young, R. M.; Neumark, D. M. Dynamics of Solvated Electrons in Clusters. *Chemical Reviews* **2012**, *112*, 5553–5577.

(24) Mitsui, M.; Nakajima, A.; Kaya, K. Mass Spectrometry and Photoelectron Spectroscopy of Tetracene Cluster Anions, (Tetracene)n - (n) 1-100): Evidence for the Highly Localized Nature of Polarization in a Cluster Analogue of Oligoacene Crystals. *J. Phys. Chem. A* **2007**, *111*, 9644–9648.

(25) Ando, N.; Kokubo, S.; Mitsui, M.; Nakajima, A. Photoelectron Spectroscopy of Pyrene Cluster Anions, $(Pyrene)_n$ (n=1–20). *Chemical Physics Letters* **2004**, *389*, 279–283.

(26) Burrow, P. D.; Jordan, K. D. On the Electron Affinities of Ethylene and 1,3-Butadiene. *Chemical Physics Letters* **1975**, *36*, 594–598.

(27) Galembeck, F.; Burgo, T. *Chemical Electrostatics*; Springer, 2017.

(28) Zürcher, U. Electrostatics at the Molecular Level. 2018; `http://dx.doi.org/10.1088/978-1-64327-186-6`.

(29) Suzuki, Y. In *Micro Energy Harvesting*; Briand, D., Yeatman, E., Roundy, S., Eds.; 2015; pp 149–174.

(30) Abouaf, R.; Benoit, C. Low-Energy Electron Collisions with Dichloromethane and Butadiene: Selectivity of Resonant Vibrational Excitation. *Chem. Phys.* **1990**, *144*, 407–411.

(31) Allan, M. What can Electron Impact Spectroscopy Offer to Photochemistry? Triplet States, Negative Ions and Intramolecular Alectron Transfer. *Pure Appl. Chem.* **1995**, *67*, 1–8.

(32) Itikawa, Y. Electron-Impact Vibrational Excitation of Polyatomic Molecules. *Int. Rev. Phys. Chem.* **1997**, *16*, 155–176.

(33) Fabrikant, I. I. Long-Range Effects in Electron Scattering by Polar Molecules. *Journal of Physics B: Atomic, Molecular and Optical Physics* **2016**, *49*, 222005.

(34) Allan, M. Study of Triplet States and Ahort-Lived Negative Ions by Means of Electron-Impact Spectroscopy. *J. Electron Spectrosc. Relat. Phenom.* **1989**, *48*, 219.

(35) Ranković, M.; Nag, P.; Zawadzki, M.; Ballauf, L.; Žabka, J.; Polášek, M.; Kočišek, J.; Fedor, J. Electron Collisions With Cyanoacetylene HC_3N: Vibrational Excitation and Dissociative Electron Attachment. *Phys. Rev. A* **2018**, *98*, 052708.

(36) Allan, M.; Lacko, M.; Papp, P.; Š. Matejčík,; Zlatar, M.; Fabrikant, I. I.; Kočišek, J.; Fedor, J. Dissociative Electron Attachment and Electronic Excitation in Fe(CO)5. *Phys. Chem. Chem. Phys.* **2018**, *20*, 11692.

(37) Šmídová, D.; Lengyel, J.; Kočišek, J.; Pysanenko, A.; Fárník, M. Analysis of Mixed Nitric Oxide–Water Clusters by Complementary Ionization Methods. *International Journal of Mass Spectrometry* **2017**, *421*, 144 – 149.

(38) Litman, J. H.; Yoder, B. L.; Schläppi, B.; Signorell, R. Sodium-Doping as a Reference to Study the Influence of Intracluster Chemistry on the Fragmentation of Weakly-Bound Clusters Upon Vacuum Ultraviolet Photoionization. *Phys. Chem. Chem. Phys.* **2013**, *15*, 940–949.

(39) Bobbert, C.; Schütte, S.; Steinbach, C.; Buck, U. Fragmentation and Reliable Size Distributions of Large Ammonia and Water Clusters. *The European Physical Journal D - Atomic, Molecular, Optical and Plasma Physics* **2002**, *19*, 183–192.

(40) Lengyel, J.; Pysanenko, A.; Poterya, V.; Kočišek, J.; Fárník, M. Extensive Water Clus-

ter Fragmentation After Low Energy Electron Ionization. *Chemical Physics Letters.* **2014**, *612*, 256–261.

(41) Poštulka, J.; Slavíček, P.; Fedor, J.; Fárník, M.; Kočišek, J. Energy Transfer in Microhydrated Uracil, 5-Fluorouracil, and 5-Bromouracil. *The Journal of Physical Chemistry B* **2017**, *121*, 8965–8974.

(42) Chao, J. S.; Falcetta, M. F.; Jordan, K. D. Application of the Stabilization Method to the N-2(1 2Pig) and Mg-(1 2P) Temporary Anion States. *The Journal of Chemical Physics* **1990**, *93*, 1125–1135.

(43) Simons, J. Resonance State Lifetimes from Stabilization Graphs. *The Journal of Chemical Physics* **1981**, *75*, 2465–2467.

(44) Falcetta, M. F.; DiFalco, L. A.; Ackerman, D. S.; Barlow, J. C.; Jordan, K. D. Assessment of Various Electronic Structure Methods for Characterizing Temporary Anion States: Application to the Ground State Anions of N2, C2H2, C2H4, and C6H6. *The Journal of Physical Chemistry A* **2014**, *118*, 7489–7497.

(45) Jagau, T. C.; Bravaya, K. B.; Krylov, A. I. Extending Quantum Chemistry of Bound States to Electronic Resonances. *Annu. Rev. Phys. Chem.* **2017**, *68*, 525–553.

(46) Tozer, D. J.; De Proft, F. Computation of the Hardness and the Problem of Negative Electron Affinities in Density Functional Theory. *The Journal of Physical Chemistry A* **2005**, *109*, 8923–8929.

(47) Vibert, C. P.; Tozer, D. J. Simple DFT Scheme for Estimating Negative Electron Affinities. *Journal of Chemical Theory and Computation* **2019**, *15*, 241–248.

(48) Hotop, H.; Ruf, M.-W.; Allan, M.; Fabrikant, I. In *Resonance and Threshold Phenomena in Low-Energy Electron Collisions with Molecules and Clusters*; Bederson, B.,

Walther, H., Eds.; Advances In Atomic, Molecular, and Optical Physics; Academic Press, 2003; Vol. 49; pp 85 – 216.

(49) Ando, N.; Mitsui, M.; Nakajima, A. Photoelectron Spectroscopy of Cluster Anions of Naphthalene and Related Aromatic Hydrocarbons. *The Journal of Chemical Physics* **2008**, *128*, 154318.

(50) Kammrath, A.; Verlet, J. R. R.; Griffin, G. B.; Neumark, D. M. Photoelectron Imaging of Large Anionic Methanol Clusters: $(MeOH)_n$ (n70–460). *The Journal of Chemical Physics* **2006**, *125*, 171102.

(51) Sarkas, H. W.; Arnold, S. T.; Eaton, J. G.; Lee, G. H.; Bowen, K. H. Ammonia Cluster Anions and Their Relationship to Ammoniated (Solvated) Electrons: The Photoelectron Spectra of $(NH_3)_{n=41-1100}$. *The Journal of Chemical Physics* **2002**, *116*, 5731–5737.

(52) DeLuca, M. J.; Niu, B.; Johnson, M. A. Photoelectron Spectroscopy of $(CO_2)_n^-$ Clusters with $2n13$: Cluster Size Dependence of the Core Molecular Ion. *The Journal of Chemical Physics* **1988**, *88*, 5857–5863.

(53) Shin, J.-W.; Hammer, N. I.; Johnson, M. A.; Schneider, H.; Glö, A.; Weber, J. M. An Infrared Investigation of the (CO2)n- Clusters: Core Ion Switching from Both the Ion and Solvent Perspectives. *The Journal of Physical Chemistry A* **2005**, *109*, 3146–3152, PMID: 16833642.

(54) Tsukada, M.; Shima, N.; Tsuneyuki, S.; Kageshima, H.; Kondow, T. Mechanism of Electron Attachment to van der Waals Clusters: Application to Carbon Dioxide Clusters. *The Journal of Chemical Physics* **1987**, *87*, 3927–3933.

(55) Weber, J. M. The Interaction of Negative Charge with Carbon Dioxide – Insight Into Solvation, Speciation and Reductive Activation From Cluster Studies. *International Reviews in Physical Chemistry* **2014**, *33*, 489–519.

(56) Fabrikant, I. I.; Hotop, H. Theory of Electron Attachment to CO_2 Clusters. *Phys. Rev. Lett.* **2005**, *94*, 063201.

(57) Stampfli, P. Theory for the Electron Affinity of Clusters of Rare Gas Atoms and Polar Molecules. *Physics Reports* **1995**, *255*, 1 – 77.

(58) Markland, T. E.; Ceriotti, M. Nuclear Quantum Effects Enter the Mainstream. *Nature Reviews Chemistry* **2018**, *2*, 0109.

(59) Amjadi, H. Charge Storage in Double Layers of Thermally Grown Silicon Dioxide and APCVD Silicon Nitride. *IEEE Transactions on Dielectrics and Electrical Insulation* **1999**, *6*, 852–857.

(60) Allan, M. Measurement of Differential Cross Sections for Excitation of Helium by Electron Impact Within the First 4 eV above Threshold. *J. Phys. B: Atom. Molec. Phys.* **1992**, *25*, 1559.

(61) Allan, M. Measurement of the Elastic and v = 0 $\rightarrow$ 1 Differential Electron–N_2 Cross Sections Over a Wide Angular Range. *J. Phys. B: Atom. Molec. Phys.* **2005**, *38*, 3655.

(62) Kočišek, J.; Grygoryeva, K.; Lengyel, J.; Fárník, M.; Fedor, J. Effect of Cluster Environment on the Electron Attachment to 2-Nitrophenol. *Eur. Phys. J. D* **2016**, *70*, 98.

(63) Lengyel, J.; Kočišek, J.; ; Fárník, M.; Fedor, J. Self-Scavenging of Electrons in $Fe(CO)_5$ Aggregates Deposited on Argon Nanoparticles. *J. Phys. Chem. C* **2016**, *120*, 7397–7402.

(64) Arad, B.; Hourahine, B.; Frauenheim, T. DFTB+, a Sparse Matrix-Based Implementation of the DFTB Method. *J. Phys. Chem. A* **2007**, *111*, 5678–5684.

(65) Grimme, S.; Antony, J.; Ehrlich, S.; Krieg, S. A Consistent and Accurate Ab Initio

Parametrization of Density Functional Dispersion Correction (DFT-D) for the 94 Elements H-Pu. *J. Chem. Phys.* **2010**, *132*, 154104.

(66) Ceriotti, M.; Manolopoulos, D. E.; Parrinello, M. Accelerating the Convergence of Path Integral Dynamics with a Generalized Langevin Equation. *J. Chem. Phys.* **2011**, *134*, 084104.

(67) Hollas, D.; Muchova, E.; Slavicek, P. Modeling Liquid Photoemission Spectra: Path-Integral Molecular Dynamics Combined with Tuned Range-Separated Hybrid Functionals. *Journal of Chemical Theory and Computation* **2016**, *12*, 5009–5017.

(68) Srsen, S.; Hollas, D.; Slavicek, P. UV Absorption of Criegee Intermediates: Quantitative Cross Sections From High-Level ab Initio Theory. *Phys. Chem. Chem. Phys.* **2018**, *20*, 6421–6430.

(69) Tsuneda, T.; Hirao, K. Long-Range Correction for Density Functional Theory. *Wiley Interdisciplinary Reviews: Computational Molecular Science* **2014**, *4*, 375–390.

(70) Vydrov, O. A.; Scuseria, G. E. Assessment of a Long-Range Corrected Hybrid Functional. *The Journal of Chemical Physics* **2006**, *125*, 234109.

(71) Muchová, E.; Slavíček, P. Beyond Koopmans' Theorem: Electron Binding Energies in Disordered Materials. *Journal of Physics: Condensed Matter* **2018**, *31*, 043001.

(72) Baer, R.; Livshits, E.; Salzner, U. Tuned Range-Separated Hybrids in Density Functional Theory. *Annual Review of Physical Chemistry* **2010**, 85–109.

(73) Janak, J. F. Proof that Delta-E-Delta-NI=Epsilon-I in Density-Functional Theory. *Physical Review B* **1978**, *18*, 7165–7168.

(74) Frisch, M. J.; Trucks, G. W.; Schlegel, H. B.; Scuseria, G. E.; Robb, M. A.; Cheeseman, J. R.; Scalmani, G.; Barone, V.; Mennucci, B.; Petersson, G. A. et al. Gaussian 09 Revision E.01. Gaussian Inc. Wallingford CT 2009.

(75) Hollas, D.; Svoboda, O.; Ončák, M.; Slavíček, P. ABIN. source code available at https://github.com/PHOTOX/ABIN.